Available online at www.sciencedirect.com
SCIENCE DIRECT®
Thermochimica Acta 419 (2004) 51–58
thermochimica acta
www.elsevier.com/locate/tca

Analytical expressions of specific heat capacities for aqueous solutions of CMC and CPE

N. Semmar, J.L. Tanguier*, M.O. Rigo

Laboratoire d'Etude et de Recherche sur le Matériau Bois, UMR INRA 1093, Université Henri Poincaré, Boulevard des Aiguillettes, BP 239, F 54506 Vandoeuvre Les Nancy Cedex, France

Accepted 12 January 2004

Available online 12 March 2004

Abstract

As previously reported, the influence of temperature and mass concentration on the specific heat capacity of two highly viscous solutions has been measured using adiabatic calorimetry. The absolute measurements were automated to operate steadily over the temperature range 290–360 K with an average heating rate of 8×10^{-4} K s^{-1}. For both solutions of carboxy-methyl-cellulose (CMC) and carboxy-poly-ethylene (CPE), the evolution of specific heat capacities with temperature is compared with that of pure water.

With CPE solutions, the increase of the temperature translated into an evolution of the C_p is comparable to the pure water with a value that varies with concentration.

For CMC solutions, we observe the same temperature behaviour for a concentration of 83 g l^{-1}. For weaker concentrations, the influence of the temperature is different.

To account for the influence of temperature and concentration parameters, we propose a correlation that facilitates the utilisation of these results corresponding to a relative error inferior to 2%.

Keywords: Adiabatic calorimeter; Specific heat capacity; Complex fluids; Polynomial correlations; Polymeric aqueous solutions

1. Introduction

Polymeric aqueous solutions, such as carboxy-methyl-cellulose (CMC) and carboxy-poly-ethylene (CPE), are widely used to simulate the rheological behaviour of highly viscous liquids. Their apparent viscosity is 10^3 to 10^4 times higher than that of water, even for very dilute solutions (1–83 g l^{-1}). Coupling both thermal and rheological studies requires the knowledge of thermophysical properties and particularly reliable specific heat capacities (C_p). But, these are not always available and are rarely reported in data bases.

As indicated in Refs. [1,2], in some earlier works, authors have simply identified the C_p of this aqueous solution type to that of pure water. In more recent works [3,4], experimental and sophisticated numerical methods have been used to determine C_p values indirectly. Nevertheless, their accuracy was estimated at less than 10%.

Thus, to achieve direct, absolute and more accurate measurements, adiabatic calorimetry was adapted to the study of CMC (18, 35, 83 g l^{-1}) and CPE (1.5, 3, 10 g l^{-1}) [5].

A second order polynomial expression allows us to link our experimental values to the temperature for each solution. From the analysis of coefficients thus obtained, we have established a more general relationship that takes into account the influence of the temperature and the concentration with a relative error inferior to 2%.

2. Apparatus performance

The spherical calorimeter used in this study was designed for solid samples at low temperatures [6], and adapted to viscous samples in the temperature range from 290 to 360 K [7]. Some details about the calorimetric device are briefly described in order to explain its performance.

The cell (Fig. 1) is centred inside a spherical shield. Its differential temperature change is controlled by a differential "T" thermocouple connected to a PID controller. Throughout

* Corresponding author. Tel.: +33-83-68-48-48; fax: +33-83-68-48-53.
E-mail address: tanguier@lermab.uhp-nancy.fr (J.L. Tanguier).

0040-6031/$ – see front matter © 2004 Elsevier B.V. All rights reserved.
doi:10.1016/j.tca.2004.01.030

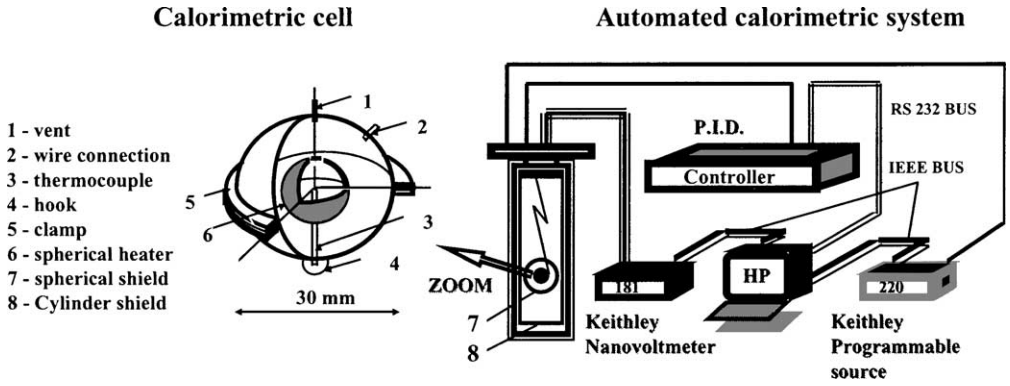

Fig. 1. Schematic view of the calorimetric device.

measurements, the difference is maintained at 0.0025 K (equivalent to 0.1 μV). The cylinder shield works under the same procedure. The temperatures of both shields are then steadily regulated with respect to the temperature measured at the centre of the cell. Consequently radiative and conductive heat losses are mostly eliminated. So, to eliminate the convective heat loss, the cell and both shields are confined inside a vacuum container with a residual pressure smaller than 10^{-2} Pa.

When computing the measurement uncertainty (Appendix A), the temperature difference between the cell and the spherical shield was considered close to 0.1 K and not to 0.0025 K. The uncertainty is then largely overestimated keeping in mind that the thermal contact between couples and surfaces is never perfect.

For the second differential thermocouple, due to the non-uniformity of the temperature on the cylinder, the temperature difference was considered equal to 1 K.

Taking into account these hypothesis in our calculation (Appendix A), the relative error induced by the different modes of thermal exchange remains very small. As shown in Fig. 2, the maximal relative error on thermal capacities of the liquid samples is inferior to 0.5%.

As shown in Fig. 3, the uncertainty induced by evaporation through the vent increases versus temperature. Consequently, all measurements were stopped at 360 K. For water and aqueous solutions, the global accuracy remains better than 2%. In order to reduce parasite mass transfer, the pressure on the sample is maintained to 1 atm. Otherwise, partial vaporisation could appear under reduced pressure.

Obviously, the effect of evaporation may be considerably reduced when using much larger cells as those employed for calibration [8]. In this case, the study of small and complex samples is eliminated and needs a higher supplied power. That leads to longer heating and stabilisation times. Notice that the ratio C_1/C_0 (C_0 and C_1 are, respectively, the absolute heat capacities of the empty and the filled calorimeter cell) is an important parameter in adiabatic calorimetry despite the reliability of the PID controller. It is approximately equal to 3.0 in this case, versus 0.2–1.0 in the case of micro-cells.

Concerning control, we have used our apparatus to measure the specific heat capacity of known substances: pure water, glycerol and paraffin.

For the pure water, the comparison of our experimental values with those published [9] shows a maximal error of 0.5% (Appendix B, Figure a).

For the glycerol (PROLABO pure to 98%), our values present a maximum gap of 2% compared to values of Ref.

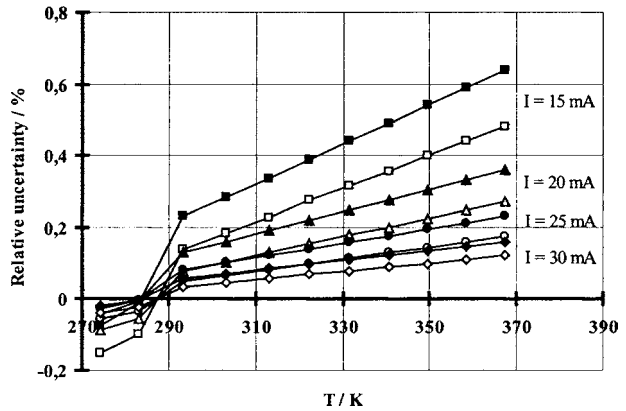

Fig. 2. Parasite heat transfer: relative uncertainty vs. temperature and current intensity (heating rate).

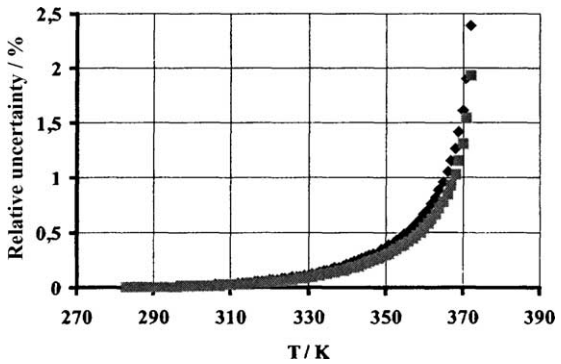

Fig. 3. Parasite mass transfer: relative uncertainty vs. temperature and current intensity (heating rate).

[10] (Appendix B, Figure b). More, against measurement with a "SETARAM" DSC calorimeter allows to validate the results.

To finish, we have tested our calorimeter with a paraffin wax "Prolabo 52–54 °C". The interest of this measure is to insure the feasibility and the reproducibility of measures for non-linear specific heat behaviour. With three series of measure, we observe a first anomaly between 300 and 313 K and a second anomaly begins at 316 K and reaches a maximum value to 324.26 K according to Delaunay [11]. Three series of measures have confirmed the reproducibility of our measures (Appendix B, Figure c).

3. Polymeric aqueous solutions

The CMC solutions are widely used to simulate the particular case of "pseudo-plastic" behaviour. In aqueous solution, CMC has disordered and tangled macromolecular chains called "static spheres" and is slightly basic.

The CMC granules are furnished by Prolabo and have an average molar mass of $2.5 \times 10^5\,\mathrm{g\,mol^{-1}}$. The degree of substitution is ranging from 65 to 95%. The solution is obtained by dissolution of granules in distilled water and exhibits a very high apparent viscosity (10^3 times higher than water) even for low mass concentration (5–35 $\mathrm{g\,l^{-1}}$).

The CPE solutions are usually used to simulate the "plastic" behaviour of complex fluids. Before being dissolved in water, the CPE resins (940 BF Goodrich Company) show a complex texture of strongly rolled balls and have an average molar mass of $2.4 \times 10^6\,\mathrm{g\,mol^{-1}}$. To prepare a gel solution, these resins must be dispersed in water with moderate stirring. Then the solution must be neutralised with a base.

Consequently, its apparent viscosity increases strongly due to the development of negative charges on the polymer axis [12]. The apparent viscosity rises to 10^4 to 10^5 times that of water. Secondary binding forces of ionic origin are induced inside the gel. The pH is between 6 and 8.

Before starting calorimetric measurements, two essential operations must be strictly followed: the filling and the baking of the calorimeter cell. A covering technique was applied separately for both detachable parts of the cell and the heating element. Then, the cell was baked for 2 h at 50 °C in order to reduce the degassing phenomenon. Without this last operation measurements are seriously affected by the heat loss induced by residual degassing. The number of gas bubbles increases with increasing apparent viscosity. The baking time should be more important for gel solutions such as CPE.

4. Measurements

As published elsewhere for adiabatic calorimetry [5], $C_p(T)$ values are usually obtained using the following expression:

$$C_p(T) = \frac{1}{m}[C_1(T) - C_0(T)] \quad (1)$$

where m is the mass of the sample.

$C_0(T)$ is the heat capacity of the empty cell. It is determined by direct measure for different intensities of heating current in the admissible value range (0–30 mA). To facilitate the exploitation of these results, the corresponding values are then smoothed using a second order polynomial correlation, such as

$$C_0(T) = -0.32T^2 + 45T + 18\,600 \quad (2)$$

When the cell is filled, we obtained $C_1(T)$ without smoothing the corresponding values. For each experimental point $C_1(T)$, the $C_p(T)$ is calculated at the mean temperature $(T_i + T_{i+1})/2$ of the working range.

A calculation example is detailed in Fig. 4 for the 18 $\mathrm{g\,l^{-1}}$ CMC solution. The total of results are regrouped in table figuring in Appendix A.

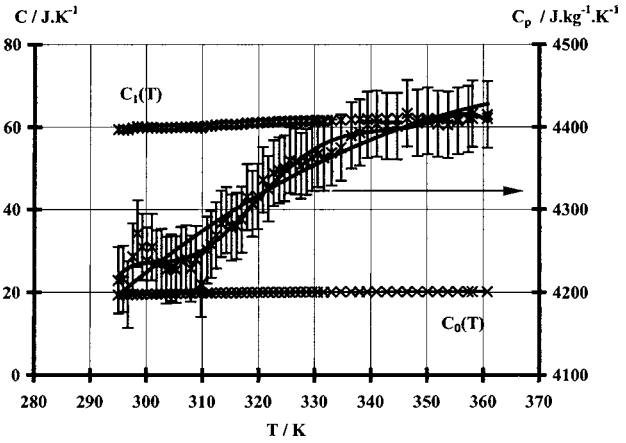

Fig. 4. Example of $C_p(T)$ determination in the case of 18 $\mathrm{g\,l^{-1}}$ CMC solution.

5. Results

Fig. 5 gives the specific heat capacity versus temperature and concentration for the CMC and CPE solutions. All values steadily increase with temperature.

For the three CPE solutions and the 83 $\mathrm{g\,l^{-1}}$ CMC solution, we observe that the temperature dependency of the specific heat evolution versus the temperature is similar and it could be compared to that of the pure water.

On the other hand for 18 and 35 $\mathrm{g\,l^{-1}}$ CMC solutions, the temperature dependency of C_p is slightly different.

First step, we use the Microsoft excel solver to describe the C_p evolution versus temperature. For each solution, values are correlated with temperature using a second order polynomial correlation, such as

$$C_p(T) = A(T - T_0)^2 + B(T - T_0) + C \quad (3)$$

where $T_0 = 273.15$ K.

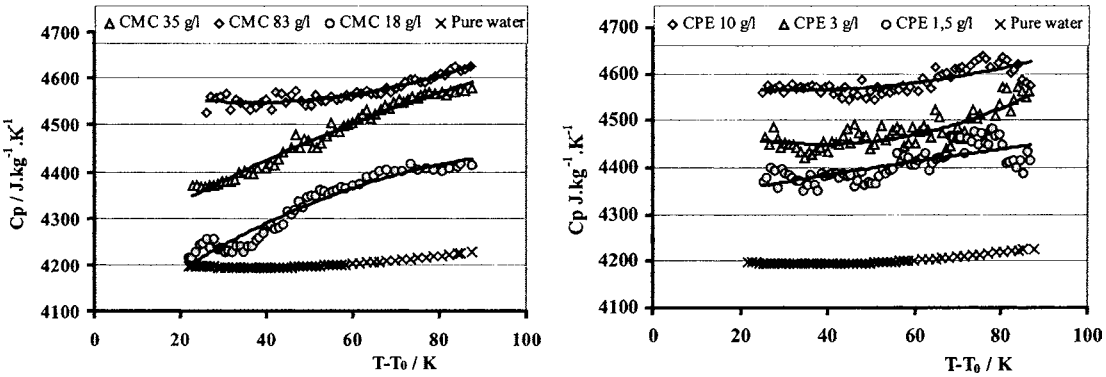

Fig. 5. C_p curves vs. temperature and mass concentration for CMC and CPE solutions.

We determinate the A, B, C coefficients using a "tangent" approach with a linear extrapolation from a tangential vector. The algorithm used for each iteration resorts to a typical Newton method with a level control of solution precision of 0.000001 and a convergence of 0.001. The determination coefficient R^2 is estimated with the following:

$$R^2 = 1 - \frac{\mathrm{SSE}}{\mathrm{SST}}, \quad \mathrm{SSE} = \sum_{i=1}^{n} (C_{p\,\mathrm{mes}} - C_{p\,\mathrm{cal}})^2,$$

$$\mathrm{SST} = \left(\sum_{i=1}^{n} C_{p\,\mathrm{mes}}^2\right) - \frac{\left(\sum_{i=1}^{n} C_{p\,\mathrm{mes}}\right)^2}{n}$$

The coefficients A, B, C and the correlation coefficient R^2 are summarised in Table 1. They enable to obtain the mean slopes, $\overline{\partial C_p}/\partial T$ for $290\,\mathrm{K} < T < 360\,\mathrm{K}$.

The analysis of these first results shows that the mean slope for the three CPE solutions and the $83\,\mathrm{g\,l^{-1}}$ CMC solution is of similar magnitude. The regression curves are nearly parallel between them and to that of pure water. From rheological considerations, this last solution ($83\,\mathrm{g\,l^{-1}}$ CMC) may be considered sufficiently concentrated to approach a gel behaviour, meaning "plastic" behaviour as in the case of CPE.

We have therefore established a more general analytic relationship which translates both the influence of the temperature (coefficients A and B) and the concentration (coefficient C). The coefficient C gives the specific heat capacity of the solutions at $T_0 = 273.15\,\mathrm{K}$. It can be therefore express as a function of $C_p(T_0)$ of the pure water and the X concentration in polymer of the solution. In the case of CPE solutions, we obtain then:

$$C = C_p(T_0)\left[1 + 0.1\left(\frac{DX}{1+DX}\right)\right] \tag{4}$$

with $D = 0.38$ for CPE solutions and $D = 0.035$ for $83\,\mathrm{g\,l^{-1}}$ CMC solution.

The analytic expression that we propose becomes

$$C_p(T, X) = A(T - T_0)^2 + B(T - T_0) + C_p(T_0)\left[1 + 0.1\left(\frac{DX}{1+DX}\right)\right] \tag{5}$$

with $A = 0.015$, $B = -0.2$, $D = 0.38$ for CPE solutions, $D = 0.035$ for $83\,\mathrm{g\,l^{-1}}$ CMC solution.

When the concentration of the CMC is inferior to $83\,\mathrm{g\,l^{-1}}$, the curves present a different slope that is also notified for another CMC solutions in Ref. [4]. So, we propose a relationship of the same type (4) with an opposite sign for the A coefficient and with different D coefficients:

$A = -0.015$, $\quad B = 5.45$,

$D = -0.013$ for $18\,\mathrm{g\,l^{-1}}$ CMC solution,

$D = 0.001$ for the $35\,\mathrm{g\,l^{-1}}$ CMC solution

Table 1
Polynomial coefficients and mean slopes of the C_p curves using Eq. (1)

	Pure water	CMC			CPE		
		$18\,\mathrm{g\,l^{-1}}$	$35\,\mathrm{g\,l^{-1}}$	$83\,\mathrm{g\,l^{-1}}$	$1.5\,\mathrm{g\,l^{-1}}$	$3\,\mathrm{g\,l^{-1}}$	$10\,\mathrm{g\,l^{-1}}$
A ($\mathrm{J\,kg^{-1}\,K^{-1}}$)	0.015	−0.032	−0.015	0.0317	0.0495	0.0455	0.0564
B ($\mathrm{J\,kg^{-1}\,K^{-2}}$)	−1.145	6.953	5.441	−2.366	−3.331	−3.548	−4.771
C ($\mathrm{J\,kg^{-1}\,K^{-3}}$)	4215.6	4061.6	4231.2	4592	4431.6	4518.8	4660.9
Mean slope	0.31	3.459	3.276	1.629	1.397	1.666	1.327
R^2	1	0.938	0.973	0.868	0.823	0.6814	0.833
Maximal relative error (%)	±0.68	±0.75	±0.5	±0.5	±0.8	±1	±0.9

Validity area: $20\,^\circ\mathrm{C} < T < 80\,^\circ\mathrm{C}$.

Definitive curves are given in Appendix C. They allow to visualise bars of uncertainty corresponding to ±0.5%.

Basically, in several gels it is usual to notice some transitions known as "gel–solution" transition. However, despite the gel state of CPE solutions, no expected "C_p anomaly" is detectable at 360 K. This surprising amorphous behaviour is probably due to significant molecular interactions. The high values of their apparent viscosities tend to confirm this. Contrarily to the gels exhibiting a "gel–solution" transition as gelatines, it is possible to measure the viscosities of CPE solutions without "crumbling" their texture. Moreover, adding soda often induced non-negligible ionic bonding, whereas in gelatines the gel "network" is obtained naturally. This is a fundamental difference between "physical gels" like gelatines, and "chemical gels" such as CPE.

The relative error (%) between experimental $C_{p\,\mathrm{exp}}$ and $C_{p\,\mathrm{cal}}$ values from Eq. (3) is given in Fig. 6. Here the relative error is given by

$$\mathrm{ER}\ (\%) = \frac{100(C_{p\,\mathrm{exp}} - C_{p\,\mathrm{cal}})}{C_{p\,\mathrm{exp}}}$$

In all cases, the relative error (%) between experimental and analytical values (from Eq. (4)) is inferior to 1%.

By adding the systematic error of +0.5% induced by our equipment (case of pure water), we can therefore conclude that the proposed analytic expression renders account of the phenomenon with a maximal relative error of 1.5%.

Even for the low values of polymeric solution mass concentration, we cannot regard their C_p as equal to that of pure water. Considering the C_p of pure water $C_p(H_2O)$ only, induces a relative difference as high as 8%.

More, the computation of weighted values as preconised by several authors [2] (i.e. $C_{p\,\mathrm{w}} = \%_{\mathrm{pol.}} \times C_{p\,\mathrm{pol.}} + \%_{H_2O} \times C_{p\,H_2O}$) gives incorrect values which increase dramatically with temperature and mass concentrations as illustrated in Table 2. For this calculation, the C_p of resins ($C_{p\,\mathrm{pol.}}$) is considered equal to 1 kJ K^{-1} kg^{-1}.

Table 2
Relative difference $[(\Delta C_p/C_{p\,\mathrm{corr.}})\,\% = 100(C_{p\,\mathrm{w}} - C_{p\,\mathrm{corr.}})/C_{p\,\mathrm{corr.}}]$ between correlated and weighted values

T (°C)	CPE			CMC		
	1.5 g l^{-1}	3 g l^{-1}	10 g l^{-1}	18 g l^{-1}	35 g l^{-1}	83 g l^{-1}
20	3.2	5.9	8.2	0.7	5.3	13.4
30	3.5	5.4	7.8	1.8	6.2	13.1
40	3.6	5.2	7.5	2.7	7.0	12.9
50	3.7	5.1	7.2	3.4	7.6	12.8
60	3.8	5.0	6.9	3.9	8.1	12.7
70	3.7	5.2	6.7	4.2	8.4	12.8
80	3.5	5.4	6.5	4.2	8.7	12.8
90	3.3	5.8	6.4	4.1	8.8	13.0

6. Discussion

Working with dilute solutions, the partial molar heat capacity at infinite dilution ($\bar{C}^0_{p,\mathrm{S}}$) may be approximated by the computation of the solution heat capacity change divided by solute molar change. Explicitly [13]:

$$\bar{C}^0_{p,\mathrm{S}} = \lim_{N_\mathrm{S}\to 0}\left(\frac{\partial C_p}{\partial N_\mathrm{S}}\right)_{T,P,N_\mathrm{W}} \cong \frac{C_p(T,P,N_\mathrm{W},N_\mathrm{S}) - C_p(T,P,N_\mathrm{W})}{N_\mathrm{S}} \quad (6)$$

where N_S and N_W are, respectively, the number of molecules (or moles) of solute and water.

Resulting values as a function of temperature and solute molar fraction ($N_\mathrm{S}/(N_\mathrm{S}+N_\mathrm{W}) \approx N_\mathrm{S}/N_\mathrm{W}$) are illustrated in Fig. 7.

As a first observation, the partial molar heat capacity at infinite dilution ($\bar{C}^0_{p,\mathrm{S}}$) decreases when increasing molar fraction. In other words, increasing the number of solute molecules induces a weaker molecular (or molar) internal energy change. Both number and magnitude of

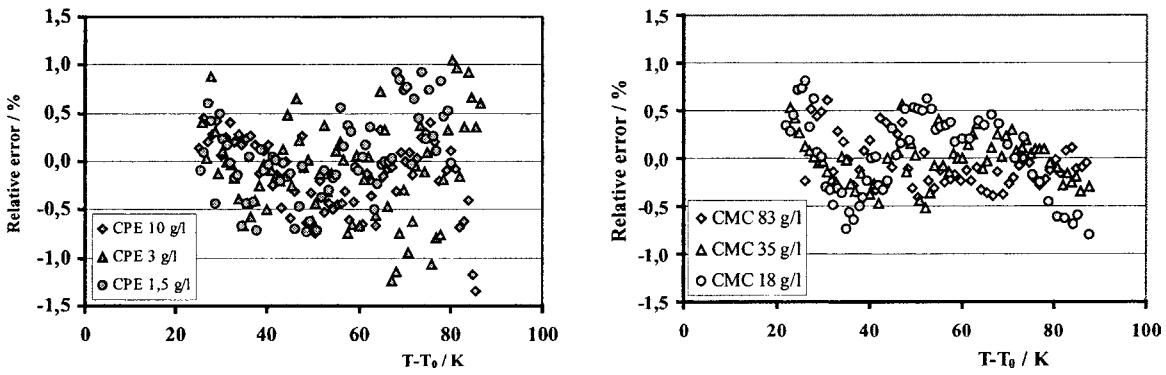

Fig. 6. Relative error vs. temperature for CMC and CPE solutions.

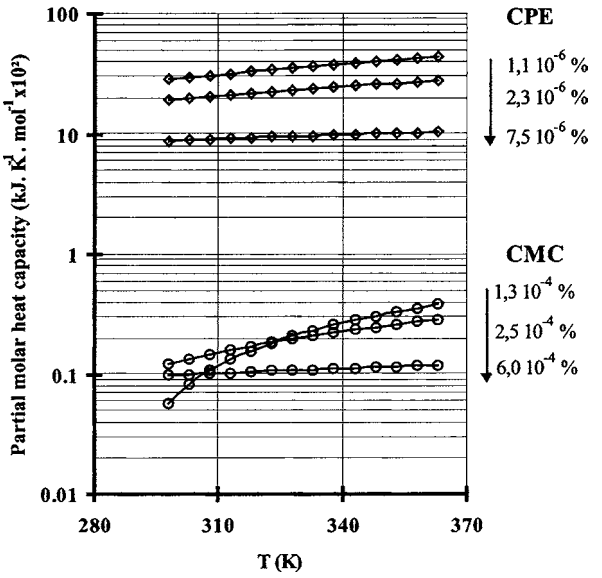

Fig. 7. ($\bar{C}^0_{p,S}$) vs. temperature and molar fraction (N_S/N_W).

molecular bonding (mainly water–polymer interactions) are in fact more important in dilute solutions. Increasing the number of macromolecules becomes more favourable to polymer–polymer interactions. Thus, the global contribution of these interactions to heat capacities increases with concentration while according to (5), ($\bar{C}^0_{p,S}$) decreases as N_S increases. Virtually, the same could be said about their apparent viscosity change versus concentration [14,15]. That means increasing apparent viscosity and decreasing the apparent viscosity change as increasing concentration.

The difference in ($\bar{C}^0_{p,S}$) between CMC and CPE solutions is also important, and may be related to the followings:

- the difference in magnitude between ionic and hydrogen bonding interactions;
- the difference in molecule sizes is more favourable to CPE macromolecules formation;
- the difference in the number of molecules that is higher in the case of CMC solutions but not favourable to their heat capacities contribution.

Otherwise, the different types of molecular interactions (i.e. van der Waals, hydrogen, ionic, etc.) induce also different values of the apparent viscosity as a function of mass fraction and size of molecules. Thus, for the same molar fraction, CPE solutions have an apparent viscosity approximately 100 times higher than for CMC solutions. Also, the apparent viscosity of CPE solutions exhibits no relevant temperature dependency contrary to viscosities for CMC [12,13]. The analysis of ($\bar{C}^0_{p,S}$) and C_p values for both solutions allows us to outline a similar qualitative behaviour between viscosities and molar partial heat capacities change with temperature and concentration.

7. Conclusion

After adaptation of the spherical calorimeter cell, C_p of viscous solutions are successfully measured using adiabatic calorimetry. A realistic estimation of the heat losses gives an overall uncertainty smaller than 0.5% below 330 K reaching 1.5% at 360 K. The specific heat capacity curves of the polymeric solutions are significantly different from that of water. For each solution, the corresponding curve is characterised by its mean slope. Globally, for all CPE solutions and the 83 g l^{-1} CMC solution, the mean slopes of specific heat capacity versus temperature curves are nearly equal. There appears to be a contribution of interactions, mainly ionic ones, in dilute solutions. However, despite the gel state of CPE solutions, no expected C_p transition was observed. The C_p values are finally correlated to temperature and mass concentration with a relative deviation close to 1.5%.

Appendix A. Measurement uncertainty calculation

The computation is based on the overall heat and mass transfer equations:

- radiation and convection between the cell and the spherical shield:

$$\Phi_r = \frac{\sigma S_c (T_c^4 - T_s^4)}{(1/\varepsilon_c) + (S_c/S_s)((1/\varepsilon_s) - 1)} \quad \text{and}$$

$$\Phi_{cv} = \frac{v+1}{2} \frac{C_v P_r}{(2\pi R T_c)^{0.5}} \frac{a_c S_c (T_c - T_s)}{1 + (S_c/S_s)(1 - a_c)}$$

- conduction and thermal fin effect between the vent, wires and the cylinder shield:

$$\Phi_{cd} = N \frac{\lambda \pi d^2}{4L} (T_c - T_{s^*}) + \lambda_t s_t \sqrt{\frac{\sigma p_t \varepsilon_t \varepsilon_{s^*}}{\lambda_t S_t}} \sqrt{\frac{2}{5} T_c^5 - 2 T_{s^*}^4 T_c + \frac{8}{5} T_{s^*}^5}$$

- mass transfer trough the vent:

$$\Phi_v = \dot{m} L_v = \frac{D_v}{R_v T} \frac{P s_t}{l_t} \ln \left[\frac{P - P_{v0}}{P - P_{sat}(T)} \right] L_v,$$

where $D_v = 2.26 \times 10^{-5} \frac{1}{P} \left(\frac{T}{273} \right)^{1.81}$

The relative uncertainty induce by parasite heat transfer is given by

$$\frac{\Phi_r + \Phi_{cv} + \Phi_{cd}}{mC_p(\Delta T/\Delta t)}$$

The relative uncertainty induce by parasite mass transfer is given by

$$\frac{\Phi_v}{mC_p(\Delta T/\Delta t)}$$

In order to reduce parasite mass transfer, the pressure on the sample is maintained to 1 atm. Otherwise, partial vaporisation could appear under reduce pressure.

Data used in this study are summarised on the following table:

λ (thermal conductivity of wires) ($W\,m^{-1}\,K^{-1}$)	200
N (number of wires)	10
L (mean length of wires) (m)	0.2
d (mean diameter of wires) (mm)	0.1
λ_t (Teflon thermal conductivity) ($W\,m^{-1}\,K^{-1}$)	0.23
l_t (length of Teflon vent) (m)	0.4
s_t (cross-section 3.2/4.8 mm) (mm^2)	10
S_t (heat exchange surface) (cm)	60.3
$\varepsilon_c = \varepsilon_s = \varepsilon_{s*}$ (total emmissivity, $\varepsilon_t = 0.7$)	0.1
R (air constant) ($J\,kg^{-1}\,K^{-1}$)	287
R_v (water vapour constant) ($J\,kg^{-1}\,K^{-1}$)	402
c_v (air isochore specific heat capacity) ($J\,kg^{-1}\,K^{-1}$)	715
S_c/S_s	0.25
a_c (accommodation coefficient)	0.5

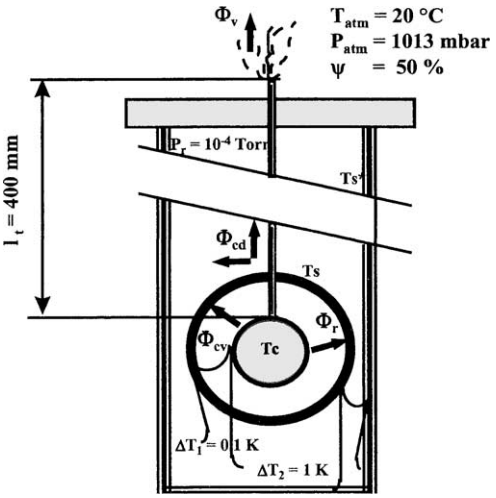

Appendix B. Comparison of experimental values with references

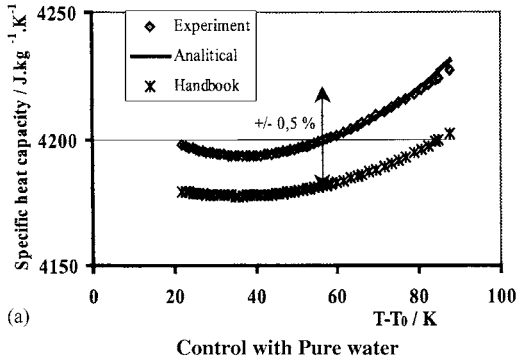

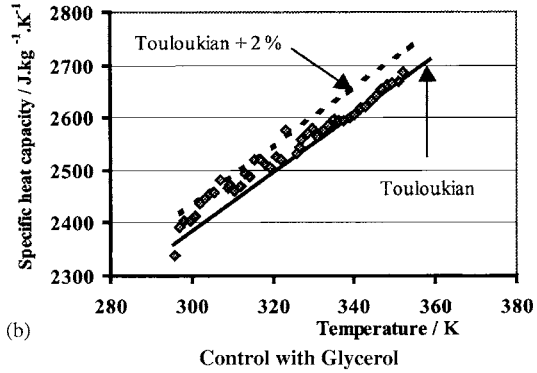

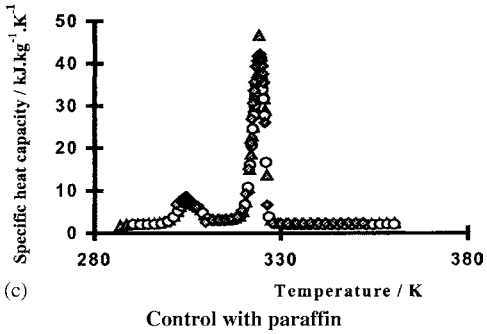

Appendix C. C_p curves versus temperature and mass concentration

For CPE solutions:

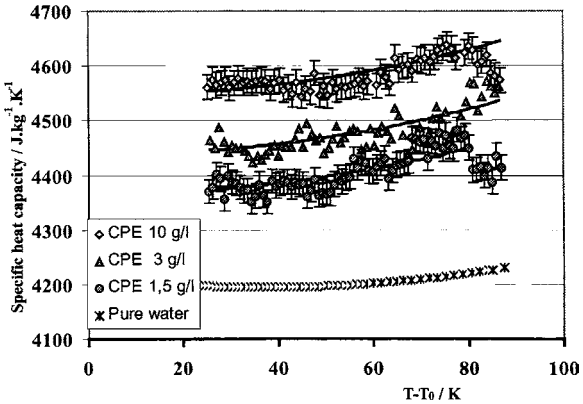

For CMC solutions:

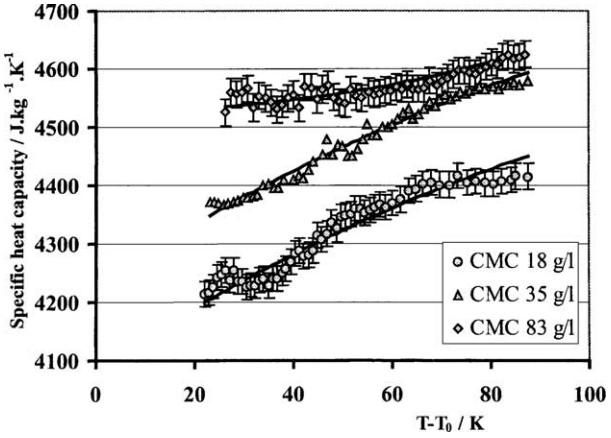

References

[1] Y.I. Cho, J.P. Hartnett, Non-Newtonian fluids in circular pipe flow, Advance in Heat Transfer, vol. 15, Academic Press, London, 1982, p. 52.
[2] A.B. Metzner, Heat transfer in non-Newtonian fluids, Advances in Heat Transfer, vol. 2, Academic Press, London, 1965, p. 357.
[3] D. Bellet, M. Singelin, C. Thirriot, Détermination des propriétés thermophysiques de liquides non-newtoniens à l'aide d'une cellule à cylindres coaxiaux, Int. J. Heat Mass Transfer 18 (1975) 1177.
[4] M. Raynaud, J. Bransier, D. Delaunay, Fluides complexes. Détermination de leur conductivité thermique et de leur capacité thermique volumique, Rev. Gén. Therm. Fr., No. 279, 1985, p. 241.
[5] N. Semmar, J.L. Tanguier, M.O. Rigo, Specific heat for carboxymethyl-cellulose and carbopol aqueous solutions, Thermochim. Acta 02DC31 (2002).
[6] J. Kleinclauss, R. Mainard, H. Fousse, A sensitive adiabatic calorimeter for measurement of low-temperature specific heats, J. Phys. E: Sci. Instrum. 10 (1977) 485–489.
[7] N. Semmar, J.L. Tanguier, J. Kleinclauss, Mise au point d'un calorimètre adiabatique utilisable avec des liquides, Int. J. Heat Mass Transfer 37 (1994) 1227–1233.
[8] G. Höhne, W. Hemminger, H.-J. Flammersheim, Differential Scanning Calorimetry, Springer-Verlag, Berlin, 1996, p. 204.
[9] Handbook of Chemistry and Physics, 46th ed., 1965–1966.
[10] Y.S. Touloukian, T. Makita, Thermophysical properties of matter, Specific Heat of Non-metallic Liquids and Gazes, no. 6, New York, 1970.
[11] D. Delaunay, Etude du couplage Convection naturelle—Conduction avec changement de phase application au stockage périodique de l'énergie, Thèse de Doctorat d'état ès-Sciences, Nantes, 1985.
[12] N'G.D. Kouamela, Etude expérimentale des écoulements en charge de fluides à seuil, Thèse INP Grenoble, Grenoble, 1991.
[13] A. Ben Aim, Water and Aqueous Solutions, Plenum Press, New York, Chapters 7 and 8, 1974.
[14] N. Semmar, Contribution à l'étude thermo-physique des fluides non-newtoniens à l'aide d'un calorimètre adiabatique original, Thèse d'Université, Nancy, 1993.
[15] C. Nouar, C. Desaubry, H. Zenaidi, Eur. J. Mech. B: Fluids 17 (1998) 875.